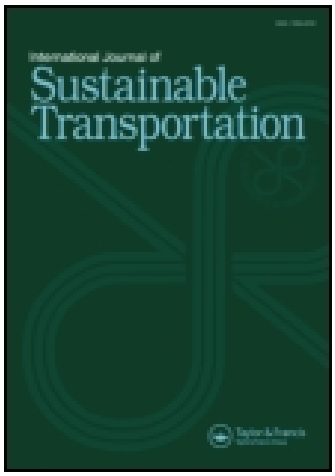

International Journal of Sustainable Transportation
Publication details, including instructions for authors and subscription information:
http://www.tandfonline.com/loi/ujst20

Traffic Congestion and Air Pollution Exposure for Motorists: Comparing Exposure Duration and Intensity

Alexander Y. Bigazzi[aa], Miguel A. Figliozzi[a] & Kelly J. Clifton[a]
[a] Department of Civil and Environmental Engineering, Portland State University, Portland, Oregon, USA

Accepted author version posted online: 11 Jul 2014.Published online: 10 Feb 2015.

International Journal of Sustainable Transportation, 9: 443–456

ISSN: 1556-8318 print/1556-8334 online
DOI: 10.1080/15568318.2013.805345

Taylor & Francis
Taylor & Francis Group

Traffic Congestion and Air Pollution Exposure for Motorists: Comparing Exposure Duration and Intensity

ALEXANDER Y. BIGAZZI, MIGUEL A. FIGLIOZZI, and KELLY J. CLIFTON

Department of Civil and Environmental Engineering, Portland State University, Portland, Oregon, USA

Received 26 April 2012, Revised 29 April 2013, Accepted 4 May 2013

This article investigates the effects of congested freeway traffic conditions on motorists' exposure to traffic-related air pollution using real-world traffic data and a framework of established emissions and dispersion models. The intent is to isolate and compare the influences of congested traffic characteristics on exposure duration and exposure intensity. Mass inhalation of carbon monoxide (CO) and nitrogen oxides (NO_x) is estimated for 45,226 simulated trips through a 14-mile congested freeway corridor. Results show that congestion increases total trip pollutant inhalation primarily through motorist delay (exposure duration), and to a lesser extent through increased concentrations (exposure intensity). The effects of varying wind and background concentration can be sufficient to obscure the influence of congestion on exposure intensity. The variability of exposure intensity due to traffic is mitigated by offsetting impacts among traffic flow, emissions rates, and pollutant dispersion. Exposure intensity increases with higher traffic flow and with lower traffic speed, but the impact of lower traffic speeds (through increased emissions rates and decreased dispersion) is smaller. The importance of exposure "hot spots" at traffic bottlenecks also increases in congestion. These findings suggest that *traffic-based* motorist exposure mitigation should focus on reducing travel duration on high-volume corridors through reduced vehicle flows (i.e., demand-side congestion mitigation). This analysis does not include non–congestion-based mitigation strategies such as cleaner vehicle engine technology or improvements in vehicle cabins, which can also reduce exposure intensity. On an individual scale, motorists can greatly reduce their own exposure during travel by, among other strategies, adjusting their departure time to less congested, lower volume periods.

Keywords: motor vehicle emissions, pollution exposure, traffic congestion

1. Introduction

Roadway traffic congestion is increasing around the world with various direct and indirect negative impacts. Heavy congestion can increase the emissions rates of air pollutants from motor vehicles, degrading urban air quality. Congestion also increases motorist delay, which extends the amount of time motorists spend in the polluted roadway environment. Exposure to traffic-related air pollution is associated with many negative health outcomes (HEI Panel 2010), but the effects of traffic congestion on travelers' exposure to air pollution are still not well documented.

Reviews by Kaur, Nieuwenhuijsen, and Colvile (2007) and Han and Naeher (2006) show broad variations in measured pollutant concentrations in different transportation environments. Most empirical research on road-user exposure is broadly aggregated, and isolating the contributions of individual factors (such as congested traffic characteristics) is difficult. Modeling of exposure in transportation environments requires integration of traffic, emissions, air quality, and traveler activity models with numerous and diverse input data. Large-scale exposure models usually treat trips as single events in static exposure environments. Some recent work has attempted to model exposure during travel in more detail by using air quality estimates that vary over the journey space and time (de Nazelle, Rodríguez, and Crawford-Brown 2009; Gulliver and Briggs 2005). However, these studies do not account for the emissions and air quality impacts of congested traffic. Other research has built traffic simulation models to predict roadside air quality (Kim, Wayson, and Fleming 2006), but traveler exposure is not explicitly considered.

This research asks the question of how freeway traffic characteristics affect motorists' exposure to pollution. Primarily, are motorists in congestion more impacted by higher exposure intensity associated with emissions from congested traffic or by longer exposure duration associated with longer travel times? Better understanding of how traffic congestion influences traveler exposure can assist in identification of traffic-based approaches for exposure mitigation. Toward that goal this paper applies existing vehicle emissions and pollutant dispersion models to simulated motorists based on real-world traffic and weather data from a 14-mile congested freeway corridor in Portland, Oregon. The value of the modeling approach is the ability to separately examine

Address correspondence to Alexander Y. Bigazzi, Department of Civil and Environmental Engineering, Portland State University, P.O. Box 751 CEE, Portland, OR 97207-0751, USA. E-mail: abigazzi@pdx.edu

the dynamics of pollution generation, exposure concentration, and exposure duration in varying traffic states. The precise estimation of exposure concentrations or mass inhalation rates is outside the scope of the study. Rather, the intent is to better understand the relative magnitude of exposure intensity and duration for motorists in congested freeway traffic. This modeling is one step in a larger study effort to quantify the impacts of traffic congestion on emissions, air quality, and human exposure.

2. Modeling Roadway Exposure

The modeling framework represents a motorized trip on a roadway corridor (which is itself part of a longer journey) as traversing a series of roadway segments (unique exposure environments). Aggregate traffic-generated pollution exposure concentrations on each roadway segment are first estimated using vehicle pollution emissions and dispersion models. Then the mass inhaled by an individual road user traveling in that environment is estimated, based on the travel speed and assumed traveler characteristics (to determine breathing rate, which is fixed in this study). This approach makes use of existing, validated models in an integrated framework.

The major components included in the modeling framework are illustrated in Figure 1. Each microenvironment (roadway segment) is represented by a homogenous set of characteristics, neglecting transitions between segments. The "Environment" inputs and models (upper box) generate estimates of Exposure Concentration, and then the "Road User" inputs and models (lower box) generate estimates of temporal and spatial mass inhalation rates for simulated travelers.

In the Environment modeling stage (upper box in Figure 1), the traffic state is represented by vehicle flow q_j (in vehicles per hour) and traffic speed v_j (in miles per hour, mph) for road segment j. Vehicle fleet, vehicle fuel, meteorology, and traffic inputs are used to estimate a pollution emissions rate e_j (in grams per vehicle-mile) with the MOVES motor vehicle emissions model from the U.S. Environmental Protection Agency (U.S. EPA 2009). Meteorology and traffic inputs are also used with the equations of the CALINE and ROADWAY pollution dispersion models to estimate a dispersion parameter d_j (in m^2/s). The emissions and dispersion estimates are combined with background concentration b_j (in g/m^3) and a vehicle penetration parameter p_j to estimate the exposure concentration on each roadway segment, c_j (in g/m^3). The penetration of air pollutant concentrations into the vehicle cabin is represented by a unit-less scaling factor p_j, which is the ratio of in-vehicle concentration to the surrounding concentration.

In the Road User modeling stage (lower box in Figure 1), assumed traveler characteristics are used to estimate a breathing rate r in m^3/hr. The breathing rate is combined with the exposure concentration estimate (c_j) to calculate the temporal inhalation rate i_j^t (in mass per unit time) over each roadway segment j. The temporal inhalation rate is combined with the travel speed s_j (in mph) to calculate the spatial inhalation rate i_j^s (in mass per unit travel distance). The breathing rate r is assumed to be constant for motorists

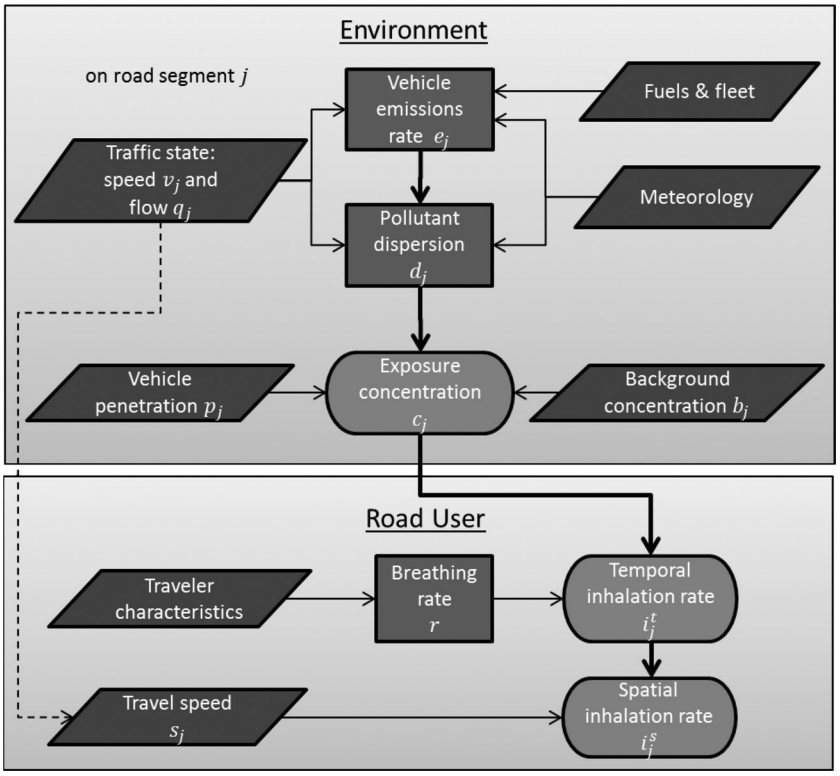

Fig. 1. The travel exposure modeling framework.

(travelers in motor vehicles—the scope of this paper). The travel speed s_j would be distinct from v_j for travelers outside of the traffic stream (bicyclists, vehicles in express lanes, etc.), but is equal to v_j for this analysis of motorists. The notation used in this paper is summarized in the appendix.

Combining the model variables (with the appropriate unit conversions), the exposure concentration c_j for a motorist on roadway segment j is the combined roadway and ambient pollution,

$$c_j = \left(\frac{e_j \cdot q_j}{d_j} + b_j\right) p_j. \tag{1}$$

The temporal mass inhalation rate is $i_j^t = c_j \cdot r$ and the spatial mass inhalation rate is $i_j^s = \frac{i_j^t}{s_j}$. The total mass inhalation I over a series of roadway segments j each of length l_j is:

$$I = \sum_j \left[i_j^s \cdot l_j\right] = \sum_j \left[\left(\frac{e_j \cdot q_j}{d_j} + b_j\right) \frac{p_j \cdot r \cdot l_j}{s_j}\right]. \tag{2}$$

The travel time on each segment is $t_j = l_j/s_j$, and the total travel time is $T = \sum_j (l_j/s_j)$. Finally, the trip-average temporal inhalation rate (in g/hr) is:

$$\overline{i^t} = I/T = \sum_j \left[\left(\frac{e_j \cdot q_j}{d_j} + b_j\right) p_j \cdot r \cdot \frac{t_j}{T}\right], \tag{3}$$

where $\frac{t_j}{T}$ is the fractional time of travel occurring on segment j. The following subsections describe the individual model components in more detail.

2.1. Traffic Flow and Speed

The traffic state variables on each segment (q_j and v_j) are drawn from archived inductive dual-loop detector data, mined from the PORTAL (Portland Oregon Regional Transportation Archive Listing) transportation data archive at Portland State University (http://www.portal.its.pdx.edu). The traffic data are aggregated to five-minute intervals, which have been shown to best approximate average freeway travel speeds (Bigazzi, Siri, and Bertini 2010; Wang and Liu 2005).

2.2. Motor Vehicle Emissions Rates

Vehicle emissions rates are modeled using the MOVES 2010 average-speed emissions model (U.S. EPA 2009), where $e_j = f(v_j)$. The average-speed approach to emissions estimation accounts for unsteady driving (accelerations) of individual vehicles by applying archetypal transient speed profiles that match a given average travel speed on a facility type. Emissions rates for CO (carbon monoxide) and NO_x (nitrogen oxides) are estimated for the year 2010 in Portland, Oregon. Where available, county-specific inputs are used (meteorology, vehicle inspection and maintenance program, fuel formulation), and national average defaults are used for other model inputs (vehicle age distributions). The vehicle fleet composition is estimated from length-based freeway vehicle classification data, with 8.7% heavy-duty vehicles (Oregon Department of Transportation 2010). The emissions estimates are for running exhaust and evaporative emissions on freeways only.

2.3. Pollutant Dispersion

Research has shown that in addition to local winds, vehicle-induced mechanical turbulence has a significant effect on turbulent dispersion around a roadway (Rao et al. 2002; Kalthoff et al. 2005). The effect of the traffic stream on dispersion varies with the traffic speed, traffic density, and size of vehicles. Unfortunately, most roadway dispersion models are intended for use well downwind of a roadway, and do not model vehicle-induced turbulence in detail (or at all). When vehicle-induced turbulence is included, it is usually insensitive to traffic characteristics, though efforts have been made to incorporate vehicle-induced turbulence into air dispersion models with more sophistication (Kanda et al. 2006).

The dispersion parameter d_j relates pollutant source strength to the concentration at a location of interest, c_j. In this study the locations of interest for motorist exposure are assumed to be at a height of 1 meter, within the travel lanes. The primary dispersion model applied here is a semi-infinite, continuous line-source Gaussian plume approximation—the basis of the CALINE roadway dispersion models (Benson 1992). Assuming steady-state dispersion conditions dominated by cross-road advection, the concentration c_j at height z due to an emissions source at height h can be calculated from the line source strength $e_j \cdot q_j$ in mass/length/time, the wind speed u, the wind angle with respect to the roadway θ, and a statistical approximation of the plume height σ_z (the standard deviation of the plume density in the vertical direction),

$$c_j = \frac{e_j \cdot q_j}{\sqrt{2\pi}\sigma_z u|\sin\theta|}\left\{\exp\left(\frac{-(z-h)^2}{2\sigma_z^2}\right) + \exp\left(\frac{-(z+h)^2}{2\sigma_z^2}\right)\right\}. \tag{4}$$

Combining factors to a single variable d_j, where $c_j = e_j \cdot q_j/d_j$, from a rearrangement of Equation 4,

$$d_j = \sqrt{2\pi}\sigma_z u|\sin\theta|/\left\{\exp\left(\frac{-(z-h)^2}{2\sigma_z^2}\right) + \exp\left(\frac{-(z+h)^2}{2\sigma_z^2}\right)\right\}. \tag{5}$$

The receptor height z, source height h, and wind speed and direction u and θ are input parameters. The remaining step for calculating d_j is estimation of the plume height σ_z, which is affected by both atmospheric and vehicle-induced turbulence. Roadway-scale atmospheric turbulence is approximated as $(0.1u)^2$ from Kastner-Klein, Berkowicz, and Plate (2000), hence the atmospheric turbulent kinetic energy (TKE) contributing to vertical dispersion is $\epsilon_z^{\text{atm}} = 0.01u^2$ in m^2/s^2. Estimation of the vehicle-induced TKE contributing to vertical dispersion $\left(\epsilon_z^{\text{veh}}\right)$ is described in the next subsection.

2.3.1. *Vehicle-Induced Turbulence*

Vehicle-induced turbulence is estimated as the variance in vertical wind speed from the vehicle wake theory of the ROADWAY dispersion model (Eskridge and Rao 1986; Rao 2002). Vehicle wake theory was also recently used for dispersion modeling in an integrated traffic and air quality simulation (Kim, Wayson, and Fleming 2006). The vehicle wake theory in ROADWAY estimates the vehicle-induced TKE at any location in the wake of a moving vehicle; TKE from multiple vehicles is combined additively by assuming independence of turbulent energy plumes. The full equations of ROADWAY are too extensive to include here, but are summarized in the appendix of Eskridge and Rao (1986). In order to apply the ROADWAY equations for aggregate traffic states (represented by q_j and v_j), an equal distribution of light-duty and heavy-duty vehicles along and among the travel lanes is assumed. Cumulative TKE from all vehicles is averaged over the roadway to generate a single estimate of the vehicle-induced vertical TKE as a function of traffic flow, traffic speed, and wind condition. A more detailed description of the calculation process follows.

In ROADWAY the TKE from a single vehicle of class λ in the set of vehicle classes Λ at location (x, y) is represented as the variance in vertical wind speed, $w'^2_{xy,\lambda}$ in m^2/s^2. The location (x, y) is based on an origin at the vehicle centroid, with x perpendicular to the direction of travel and y as the distance behind the vehicle, parallel to the direction of travel (and perpendicular to x). TKE in ROADWAY is a function of wind speed u, wind angle with respect to the roadway θ, vehicle class-average speed v_j^λ (for road segment j), and the vector of vehicle characteristics for vehicle class λ (height, width, length, and drag coefficient) $\hat{\lambda}$: $w'^2_{xy,\lambda} = f\left(u, \theta, v_j^\lambda, \hat{\boldsymbol{\lambda}}, x, y\right)$.

The total TKE on the roadway contributed by a single vehicle of class λ in lane n is

$$w'^2_\lambda = \int_{-\infty}^{\infty} \int_{W\left(-n+\frac{1}{2}\right)}^{W\left(N-n+\frac{1}{2}\right)} w'^2_{xy,\lambda} dx dy$$

in m^2/s^2, where N is the total number of lanes and W is the width of a single lane. The total TKE from all vehicles of class λ, averaged over the roadway, is

$$\frac{q_j^\lambda}{v_j^\lambda N^2 W} \sum_{n=1}^{N} w'^2_\lambda$$

where q_j^λ and v_j^λ are the λ class-specific traffic flow and speed on segment j, respectively. Combining these, the total TKE from all vehicle classes λ in the set of vehicle classes Λ, averaged over the roadway, is

$$\epsilon_z^{\text{veh}} = \sum_{\lambda \in \Lambda} \left\{ \frac{q_j^\lambda}{v_j^\lambda N^2 W} \sum_{n=1}^{N} \left[\int_{-\infty}^{\infty} \int_{W\left(-n+\frac{1}{2}\right)}^{W\left(N-n+\frac{1}{2}\right)} w'^2_{xy,\lambda} dx dy \right] \right\} \quad (6)$$

in m^2/s^2. The value of ϵ_z^{veh} with the inputs $u, \theta, v_j^\lambda, q_j^\lambda$ and N is calculated numerically using a 0.2-meter grid, a y range of 0–500 m, $W = 4$ m, and $\hat{\lambda}$ from Table 1. Assumed vehicle size and shape parameters $\left(\hat{\boldsymbol{\lambda}}\right)$ from Baumer, Vogel, and Fiedler (2005) and Wang et al. (2006) are shown in Table 1 for light-duty (LD) and heavy-duty (HD) vehicle classes ($\Lambda = \{\text{LD, HD}\}$). Equal speeds across vehicle classes is also assumed: $v_j^\lambda = v_j \, \forall \, \lambda$ in Λ. Using a vehicle-class flow fraction of f_λ, $q_j^\lambda = f_\lambda \cdot q_j$. Again based on freeway vehicle classification data (Oregon Department of Transportation 2010), $f_{HD} = 0.087$ and $f_{LD} = 1 - f_{HD}$.

Table 1. Assumed vehicle parameters for estimation of traffic-induced turbulence on the roadway

	Light-duty vehicles	Heavy-duty vehicles
Drag coefficient	0.3	0.9
Vehicle height (m)	1.4	3.5
Vehicle width (m)	1.8	2.4
Vehicle length (m)	5.5	22.5

2.3.2. *Plume Height*

Combining the vehicle-induced and atmospheric turbulence, the total TKE contributing to vertical dispersion is $\epsilon_z = \epsilon_z^{\text{veh}} + \epsilon_z^{\text{atm}}$ in m^2/s^2. In order to calculate σ_z from ϵ_z, a constant vertical diffusion coefficient is assumed that is the product of the characteristic length and velocity scales of the turbulent eddies. A constant vertical diffusion coefficient implies short-term steady-state traffic and meteorology. The characteristic length and velocity scales of roadway turbulence are taken as the composite vehicle height H (calculated using 8.7% heavy-duty vehicles and as $H = 1.583$ m) and the square root of the vertical TKE (ϵ_z), respectively (Baumer, Vogel, and Fiedler 2005; Kono and Ito 1990). From Pasquill (1983) the statistical plume height can then be estimated:

$$\sigma_z = \sqrt{2\tau H \sqrt{\epsilon_z}}, \quad (7)$$

where τ is the pollutant residence time on the roadway in seconds,

$$\tau = \frac{NW + 6}{2u|\sin(\theta)|}, \quad (8)$$

with u in m/s and W in m (Benson 1992). The assumption stated above that crosswind advection dominates dispersion ensures that $u|\sin(\theta)| > 0$.

Combining Equations 5–8 and assuming a source height of $h = 0.3045$ m (ground-level emissions for LD vehicles and vehicle-height-level emissions for HD vehicles) in addition to the previous assumptions of $W = 4$ m, $z = 1$ m, and $H = 1.583$ m, d_j in m^2/s is

$$d_j = \frac{\sqrt{6.33\pi(2N+3)u|\sin(\theta)|\sqrt{\epsilon_z^{\text{veh}} + 0.01u^2}}}{\exp\left(\frac{-0.0764u|\sin(\theta)|}{(2N+3)\sqrt{\epsilon_z^{\text{veh}}+0.01u^2}}\right) + \exp\left(\frac{-0.8509u|\sin(\theta)|}{(2N+3)\sqrt{\epsilon_z^{\text{veh}}+0.01u^2}}\right)}. \quad (9)$$

with u in m/s and ϵ_z^{veh} in m^2/s^2. In addition to changing with u, θ, and N, d_j is a function of q_j and v_j through ϵ_z^{veh} (Equation 6).

The approach described here is an approximation of average conditions based on previously established methods of

estimating roadway dispersion. The intent is to account for the major influences on pollutant transport while recognizing that short-term concentrations will vary widely. Of particular note, this approach assumes a longitudinally well-mixed roadway air mass, and will likely not accurately represent an idling queue (not modeled here) where the proximity of tailpipes and following vehicles' air intakes can become a dominant factor (Clifford, Clark, and Riffat 1997; McNabola, Broderick, and Gill 2009).

2.4. Breathing Rate

Most traffic exposure research accounts for human uptake with a breathing or ventilation rate, although McNabola, Broderick, and Gill (2008) use a more complex human respiratory tract model for pollutant absorption. Pollutant uptake can become more complicated when accounting for factors such as individual physiology, nose versus mouth breathing, and pollutant compound solubility. Assuming that motorists' respiration is exogenous (not significantly impacted by traffic conditions), a constant, average breathing rate of $r = 0.66\,\mathrm{m}^3/\mathrm{hr}$ is used here, based on O'Donoghue et al. (2007), which also agrees well with Wijnen et al. (1995).

2.5. Vehicle Penetration

The penetration of pollutants into the vehicle depends on the cabin air exchange rate and air filtration system. Empirical and modeling studies have shown that p_j can vary with vehicle ventilation conditions and cabin particle filters (Bigazzi and Figliozzi 2012; Xu and Zhu 2009; Zhu et al. 2007). Others have suggested that for fine particulates and CO the vehicle shell has no effect, implying $p_j = 1$ (Kaur, Nieuwenhuijsen, and Colvile 2007). Because the cabin air exchange rate can be affected by speed (Xu and Zhu 2009), p_j could be a function of the traffic state, in which case p_j would be expected to increase with speed. But there is a lack of data on how p_j varies with speed for different pollutants, especially gases. Also, the relationship between p_j and s_j would depend on the vehicle characteristics (age, cabin size, etc.) and ventilation conditions (windows, fan, etc.).

Given the uncertainty in vehicle penetration of pollutants, the primary analysis in this study neglects vehicle shell effects by assuming a constant $p_j = 1\ \forall j$. This approach estimates traffic impacts on roadway concentrations, while acknowledging that well-sealed cabins could reduce individuals' concentration levels proportionally. The possible influence of traffic effects on p_j is examined in Section 3.4 by assuming a linear relationship between p_j and v_j from Xu and Zhu (2009).

2.6. Background Concentration

In the modeling framework the background concentration b_j includes ambient concentrations and the emissions of counter-flowing and other nearby traffic. Hourly average concentrations of urban background CO and NO_x in Portland are obtained from Oregon Department of Environmental Quality (ODEQ) monitoring stations for 2010, through the Horizons web data service (George, Parra, and Sitbon 2005). The ODEQ monitoring stations are sited away from major highway facilities. NO_x estimates in ppm are converted assuming $1\,\mathrm{ppm} = 1.555\,\mathrm{mg/m}^3$($NO/NO_2$ ratio of 1).

2.7. The Effects of Congestion in the Model

The average temporal inhalation rate $\overline{i^t}$ is the exposure intensity measure in this paper, and the exposure duration is the travel time T. Exposure duration T is only affected by speed v_j (equal to s_j), while exposure intensity $\overline{i^t}$ is a function of q_j, e_j, d_j, r, p_j, b_j, and v_j (again through s_j). In turn, dispersion d_j is a function of both traffic state variables v_j and q_j, while emissions rate e_j is a function of just traffic speed v_j. Other model variables are considered exogenous to congestion (r, p_j, and b_j).

2.8. Corridor Study Data

The modeling framework is applied to estimate exposure for individual motorists over 12 months in 2010 on a 13.79-mile stretch of the I-5 northbound freeway through Portland, Oregon. Simulated motorists depart from milepost 290 on the southern end of the corridor every 5 minutes from 6 a.m. until 8 p.m. on each day. Their exposure is modeled over 15 freeway segments up to milepost 304, with lane widths of 4 m. The freeway segments are delineated by the midpoints between traffic sensors, which are approximately 1 mile apart on average. Although a High Occupancy Vehicle (HOV) lane exists at the end of the corridor, it is not used by the simulated motorists. The emissions and dispersion impacts of the HOV lane vehicles are included (with HOV lane-specific traffic speeds). Regional wind data (hourly average speed and direction) for dispersion estimates are obtained from the same ODEQ monitoring stations as the background concentrations. A minimum wind angle to the road of 15° is used ($15° \le \theta \le 345°$ and $15° \le |180° - \theta| \le 345°$) because of the model assumption that cross-road advection dominates pollutant dispersion.

Two different exposure estimates are made: method (1) uses real-world traffic, wind, and background concentration data and method (2) uses only varying traffic data (q_j and v_j) and fixes the exogenous factors (wind condition and background concentrations: u, θ, and b_j). Thus, method (1) gives more realistic estimates, while method (2) enables investigation of traffic effects alone. For method (2), wind is assumed to be 3 m/s at a bearing of 135° and background concentrations are assumed to be $457\,\mu\mathrm{g/m}^3$ for CO and $25\,\mu\mathrm{g/m}^3$ for NO_x (based on the ODEQ data). The factors that are held invariant in method (2)—background concentrations b_j, wind u and θ, breathing rate r, vehicle penetration p_j—will certainly contribute to varying individual pollution exposures, but they are held constant in order to address the research question more directly: how do changing traffic conditions impact exposure duration and intensity for motorists?

3. Results

Of the 61,320 potential simulated trips for the year, only 45,226 complete trips (74%) are modeled because of incomplete or low-quality traffic data (the unmodeled trips are approximately evenly spread over the day and across the week). Table 2 presents a summary of the modeled trips' travel time T, mass inhalation I, exposure intensity $\overline{i^t}$, background concentration b_j, modeled dispersion parameter d_j, and modeled total emissions $e_j \cdot q_j$ in kg/hr per mile of roadway. The first three columns in Table 2 show the results using exposure estimation method (1), varying wind and background conditions, and the second three columns show the results using method (2), with fixed wind and background conditions. For values affected by the calculation method (mass inhaled I, exposure intensity $\overline{i^t}$, and dispersion d_j), the central values agree well between the two methods but the variance is notably higher by method (1) than method (2). The relative standard deviation of all the variables in Table 2 is high (around 35% of the mean or greater) except for exposure intensity and dispersion under method (2). The travel time, mass inhalation estimates, and background concentrations exhibit positive (right) skew, with larger mean than median values.

Examining exposure duration, travel times for the simulated trips average 17 min. and range from 13 to 74 min., the longer being equivalent to an average speed of just 11 mph. The relative standard deviation of exposure duration (T) is 35% of the mean, compared with a relative standard deviation of 46% of the mean for CO exposure intensity $\left(\overline{i^t}\right)$ by method (1) and just 8% of the mean for CO exposure intensity by method (2) (Table 2). At a breathing rate of $r = 0.66\,m^3/hr$, the mean values of $\overline{i^t}$ in Table 2 correspond to exposure concentrations of 608 $\mu g/m^3$ and 90 $\mu g/m^3$ for CO and NO_x, respectively. The range of trip-average exposure concentrations by method (1) for CO is 24–2,999 $\mu g/m^3$ (0.02–2.6 ppm), which is toward the lower end of the ranges reported by Fruin et al. (2008), Kaur, Nieuwenhuijsen, and Colvile (2007), and Zagury, Moullec, and Momas (2000) for drivers in higher-density urban environments than Portland (London, Paris, Los Angeles, etc.). Method (1) trip-average NO_x exposure concentrations range from 13 to 468 $\mu g/m^3$, also toward the lower end of the range reported by Zagury, Moullec, and Momas (2000).

Comparing the traffic-generated pollution $\left(\frac{e_j \cdot q_j}{d_j}\right)$ to the background concentrations (b_j), a much greater share of mass inhalation is generated by the modeled traffic stream for NO_x than for CO. On average, the estimated trip inhalation of CO is only 41% greater than it would be from the background concentrations alone, while the trip inhalation of NO_x is almost five times greater than background levels. This observation is likely due to the longer lifetime of CO, which is more inert than NO and so more persistent as it disperses from roadways (Gordon et al. 2012). Atmospheric chemical transformations are not being modeled in this analysis, but will have a greater impact on NO_x than CO because of the higher reactivity of NO_x (especially important on the time scale required to reach background concentrations). With an average crosswind speed of 2.2 m/s, the average residence time in a three-lane roadway from this analysis (Equation 8, which is not pollutant-dependent) is only 6.5 seconds, so neglecting chemical reactions is unlikely to have a large effect on the results. Trip inhalation ranges up to 36 times greater than background levels for CO and up to 31 times greater for NO_x by the method (1) estimates.

A high correlation is observed between the two pollutants: total trip inhalations of CO and NO_x have correlation coefficients of 0.85 by method (1) and 0.99 by method (2). This is not surprising; without modeling atmospheric chemistry, only different shapes of the emission-speed relationships $e_j = f(v_j)$ differentiate the gases by method (2). Differing background concentrations are also relevant for method (1). The correlation of total trip inhalation for each gas between estimation methods is lower: 0.64 for CO and 0.73 for NO_x. Given the strong correlation between the pollutants, the following results focus on CO because the findings related to traffic effects are essentially the same and the unmodeled chemical transformation of CO will be lesser.

3.1. Exposure and Congestion

Addressing the first objective of this research, total trip mass inhalation of both CO and NO_x increases with travel time,

Table 2. Summary of modeled trip exposures

	(1) Varying wind and background			(2) Fixed wind and background		
	Mean	Median	Std. deviation	Mean	Median	Std. deviation
Travel time T (min)	17.44	14.95	6.16	—	—	—
CO inhaled I (μg)	118.69	97.87	75.44	116.76	95.95	54.36
CO exposure intensity $\overline{i^t}$ (μg/hr)	401.58	359.56	185.61	392.52	386.13	31.45
CO background b_j (μg/m^3)	456.68	395.02	258.73	—	—	—
NO_x inhaled I (μg)	18.12	14.10	13.28	17.15	13.35	11.10
NO_x exposure intensity $\overline{i^t}$ (μg/hr)	59.65	53.27	28.66	55.57	53.67	12.29
NO_x background b_j (μg/m^3)	25.09	16.98	25.23	—	—	—
Dispersion d_j (m^2/s)	9.87	9.52	3.54	9.72	9.98	1.17
CO emissions, $e_j \cdot q_j$ (kg/hr/mi)	7.39	7.58	2.98	—	—	—
NO_x emissions, $e_j \cdot q_j$ (kg/hr/mi)	3.21	3.31	1.26	—	—	—

indicating that trips made in congestion subject motorists to greater pollution uptake. Linear regression of CO and NO_x mass inhalation I (μg) on travel time T (min) produces the coefficients, standard errors, and R^2 values shown in the first two rows of Table 3 (not constrained to pass through the origin). All four are significant at $p < 0.01$. Mass inhalation increases with travel time similarly by both methods, but the statistical fit (R^2) is much poorer by method (1) because of greater variability. The third and fourth rows of Table 3 show the same regression but only for the traffic-generated pollution inhalation (subtracting the background concentrations, i.e., I with $b_j = 0$). Here, again, total mass inhalation increases in congested conditions with higher T, and all four are significant at $p < 0.01$.

The bottom two rows in Table 3 show the results of similar regressions of CO and NO_x exposure intensity ($\overline{i^t}$ in μg/hr) on travel time (T in min). These estimated coefficients indicate that exposure intensity also increases in congestion for both CO and NO_x. The coefficient estimates are again significant at $p < 0.01$, but the explained variance in the models (indicated by R^2) is very low for exposure intensity by method (1). This poor fit illustrates the degree to which traffic effects can be obscured by wind and background concentration variability and motivates the inhalation modeling in this study using fixed meteorology and background concentrations to eliminate those exogenous sources of variance.

The spatial distribution of mass inhalation is of interest for exposure "hot spots." For many high-exposure motorists, the mass inhalation is concentrated in several locations along the corridor, coinciding with traffic bottlenecks. On the average simulated trip, one roadway segment generates three times greater inhalation than the average of the rest of the trip. The uneven spatial distribution of exposure is intensified in congestion, as the single highest-exposure segment on each trip increases its share of the total trip inhalation by 0.7% for each additional minute of trip travel time (that single segment represents, on average, 17% of the total exposure). Because total trip inhalation is greater in congestion (Table 3), the importance of these exposure "hot spots" on the corridor is intensified.

3.2. Comparing Exposure Duration and Intensity

The total mass inhalation is the product of the exposure intensity and exposure duration, $I = \overline{i^t} \cdot T$. In order to address which one is the primary influence on total inhalation, single-factor analysis of variance is performed to calculate the explained sum of squares associated with each of exposure intensity and exposure duration. The results are that 39% of the variance in I of CO by method (1) is explained by duration (T) alone, while 64% is explained by intensity ($\overline{i^t}$) alone. In contrast, 99% of the variance in I of CO by method (2) is explained by duration alone, while 74% is explained by intensity alone. The percentages do not sum to 100% because of a correlation between exposure intensity and travel time (Table 3).

Similar analysis of variance for NO_x inhalation results in 50% of the variance in I by method (1) explained by duration alone, and 68% explained by intensity alone. In contrast, 96% of the variance in I by method (2) is explained by duration alone, and 76% is explained by intensity alone. Thus, in terms of traffic effects as modeled by method (2), exposure duration (T) is the primary factor determining pollutant inhalation over a trip (I). Although exposure duration is the primary path of *traffic congestion's* influence on total exposure, variability in exposure intensity ($\overline{i^t}$) due to exogenous factors (wind and background concentrations) is the larger determinant of inhalation (I) as modeled by method (1). Exposure intensity will also vary with other exogenous factors not included in the model (e.g., the vehicle fleet composition), although this analysis focuses on the effects of congestion (Section 2.7).

As an illustration of the importance of exposure duration in congestion, consider an alternative hypothetical motorist who traverses the same road segments at the same times as the motorists in congestion, but at a constant free-flow speed of $s_j = 60$ mph, for 14 minutes total travel time (a free-flowing HOV lane, for example, where travel speed s_j is independent of traffic speed v_j). These motorists have the same exposure concentrations and temporal inhalation rates i_j^t as the motorists experiencing delay, but shorter (or similar) exposure durations.

Figure 2 shows total trip CO inhalation for both the hypothetical constant-speed motorists and the simulated motorists experiencing delay, plotted against the average corridor traffic speed (as experienced by the delayed motorist). The plot on the left of Figure 2 uses the method (1) inhalation rate estimates with varying wind and background concentrations and the plot on the right uses the method (2) estimates. The extremely high trip inhalations at low

Table 3. Mass inhalation and congestion: Regressions of trip CO and NO_x total inhalation and inhalation rates on minutes of travel time

	(1) Varying wind and background			(2) Fixed wind and background		
N = 45,226	Unit change per minute T	Std. Error	R^2	Unit change per minute T	Std. Error	R^2
CO inhaled (μg)	7.69	0.0450	0.39	8.78	0.0043	0.99
NO_x inhaled (μg)	1.51	0.0073	0.50	1.76	0.0018	0.96
Traffic-generated CO inhaled (μg)	3.32	0.0125	0.61	3.76	0.0043	0.94
Traffic-generated NO_x inhaled (μg)	1.31	0.0052	0.59	1.48	0.0018	0.94
CO exposure intensity (μg/hr)	3.16	0.1416	0.01	4.18	0.0138	0.67
NO_x exposure intensity (μg/hr)	1.19	0.0214	0.07	1.57	0.0058	0.62

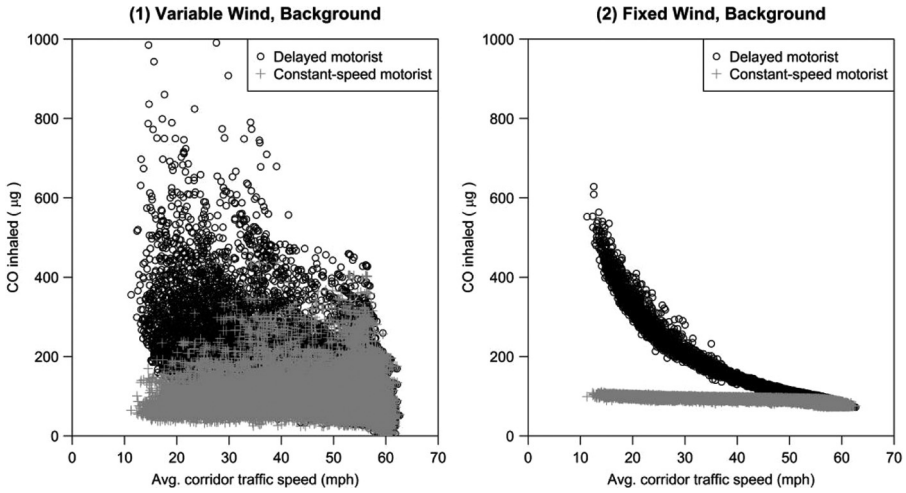

Fig. 2. Comparison of total trip CO inhalation for delayed and constant-speed motorists at different corridor traffic speeds; without delay effects, the inhalation increase in congestion is slight.

traffic speeds (i.e., during congestion) for the delayed motorist almost disappear for the constant-speed motorist. Although CO exposure intensity does tend to be higher when traffic speeds are lower, without delay the inhalation increase in congestion is only slight. This result appears in both plots, but is most clear on the right in Figure 2 where traffic effects are isolated using method (2).

In comparison to the values in Table 3, constant-speed motorists in the otherwise same exposure conditions experience trip CO inhalation increases of only 0.35 µg per additional minute of travel time by method (1) and 0.56 µg per minute of travel time by method (2), reductions of 95% and 94% from the first row of Table 3, respectively. These estimates are significant at $p < 0.01$, but while R^2 for method (2) is 0.49, the R^2 for method (1) is only 0.003. Thus, outside the effect of delay, varying wind and background concentration conditions are sufficient to obscure the impact of traffic conditions on inhalation.

It might be noted that although they are similar measures, the statistical fit between T and a constant-speed motorist's CO inhalation is poorer than between T and CO exposure intensity $\overline{i^t}$ in Table 3. The reason for this difference is that $\overline{i^t}$ is affected by the distribution of travel time among segments of the corridor. As described in Section 3.1, there are bottleneck locations on the corridor with higher exposure intensity. During congestion, when the bottlenecks are active, a disproportionate amount of time is spent on those high-exposure-intensity sections. The constant-speed motorist only measures the effects of varying on-road pollution concentrations, while $\overline{i^t}$ reflects the effects of congestion on both roadway concentrations and the distribution of exposure duration.

3.3. *Relationships Among Model Variables*

This section examines the different model components to better understand how traffic conditions impact exposure. Table 4 shows linear correlation coefficients between CO and NO_x exposure intensity at the segment level $\left(i_j^t\right)$ and the traffic flow and traffic speed variables q_j and v_j. The correlations reveal that traffic flow q_j has a stronger statistical linear relationship to all four exposure intensity variables than traffic speed v_j. The strong positive effect of flow on exposure intensity means that a fixed amount of delay is less harmfully experienced on a lower-flow section.

As explained in Section 2.7, exposure duration is only affected by the travel speed s_i (here the same as traffic speed v_j), while exposure intensity is influenced by all the other model variables. This is important because the variables are correlated among themselves, which can have offsetting effects on exposure intensity. Table 5 shows correlation coefficients between model variables at the segment level for CO. As an example, consider that dispersion d_j is positively correlated with traffic flow q_j (also indicated by Equation 6). As can be seen in Equation 3, a simultaneous increase in these two variables will have offsetting effects on exposure intensity. A negative correlation between

Table 4. Correlation coefficients between traffic variables and exposure intensity (CO and NO_x inhalation rates)

	(1) Varying wind and background		(2) Fixed wind and background	
N = 678,390	CO exposure intensity (µg/hr)	NO_x exposure intensity (µg/hr)	CO exposure intensity (µg/hr)	NO_x exposure intensity (µg/hr)
Traffic flow q_j (veh/hr)	0.18	0.72	0.40	0.77
Traffic speed v_j (mph)	−0.15	−0.62	−0.28	−0.58

Table 5. Correlation coefficients between model variables for CO

N = 678,390	Traffic flow q_j	Traffic speed v_j	Emissions rate e_j	Dispersion (1) d_j	Dispersion (2) d_j	Wind speed u	Background conc. b_j
Traffic flow q_j	1.00						
Traffic speed v_j	−0.01	1.00					
Emissions rate e_j	−0.06	−0.77	1.00				
Dispersion (1) d_j	0.28	0.13	−0.09	1.00			
Dispersion (2) d_j	0.74	0.62	−0.50	0.32	1.00		
Wind speed u	0.02	−0.04	0.04	0.68	0.00	1.00	
Background conc. b_j	0.04	−0.05	0.00	−0.17	0.00	−0.17	1.00

emissions rate e_j and traffic flow q_j (Table 5) also has offsetting effects on exposure intensity.

Figure 3 shows total emissions strength $e_j \cdot q_j/N$ in kilograms per hour per lane-mile of roadway for CO. The modeled total emissions are plotted as shaded contours on the traffic speed-flow (v_j versus q_j/N) plane; circles illustrate the locations of observed traffic states on the study corridor during 19–20 January 2010 (8,226 observations). Traffic flow is in vehicles per hour per lane (veh/hr/ln). Total emissions increase linearly with traffic flow and nonlinearly with speed at very high and low travel speeds, based on the form of $e_j = f(v_j)$.

Heavily congested periods in Figure 3 with speeds below 20 mph have lower traffic flows than mildly congested periods, as can be expected from traffic flow theory (May 1989). Thus, the highest total emissions are on moderately congested road segments with high flows and speeds above 25 mph. The most heavily congested segments (as indicated by traffic speed) have the highest emissions rates per vehicle-mile e_j, but their lower vehicle flows q_j offset the higher marginal emissions. Low vehicle flows cause queuing upstream, so congestion will displace some emissions to upstream segments and later time periods. But at the location of interest, Figure 3 shows that the time periods with the lowest speeds (and highest emissions rates) are not necessarily those with the most total emissions.

Figure 4 shows dispersion parameter d_j estimates as shadings on the same traffic speed-flow plane with the same illustrative traffic data as Figure 3. The modeled values of d_j use the fixed-wind conditions in method (2): 3 m/s wind at a bearing of 135 degrees, and 3 travel lanes of 4 m each. Higher traffic speeds and flows both increase d_j. In moderate levels of congestion, lower speeds offset the effect of higher flows on d_j. Increasingly severe congestion has lower dispersion estimates as both speeds and flows are reduced. Since dispersion d_j is inversely proportional to traffic-related pollutant concentrations, lower dispersion in heavy congestion will lead to higher roadway concentrations at a given emissions intensity.

Together, Figure 3 and Figure 4 demonstrate offsetting effects of traffic conditions, where the highest total emissions but also the greatest dispersion are expected in high-flow

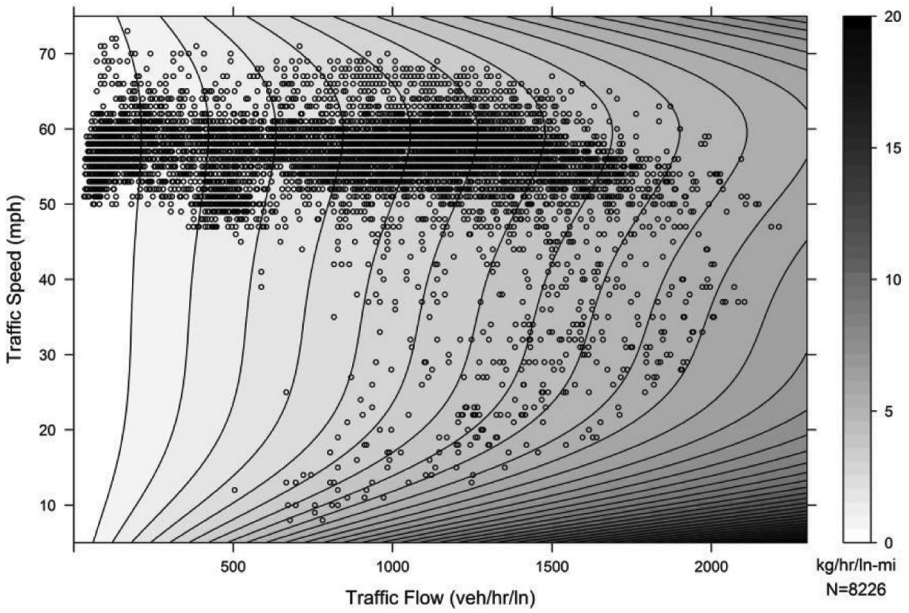

Fig. 3. Modeled total CO emissions as shading on the traffic state (speed vs. flow) plane with illustrative traffic data; total emissions are highest in moderate congestion with high flows.

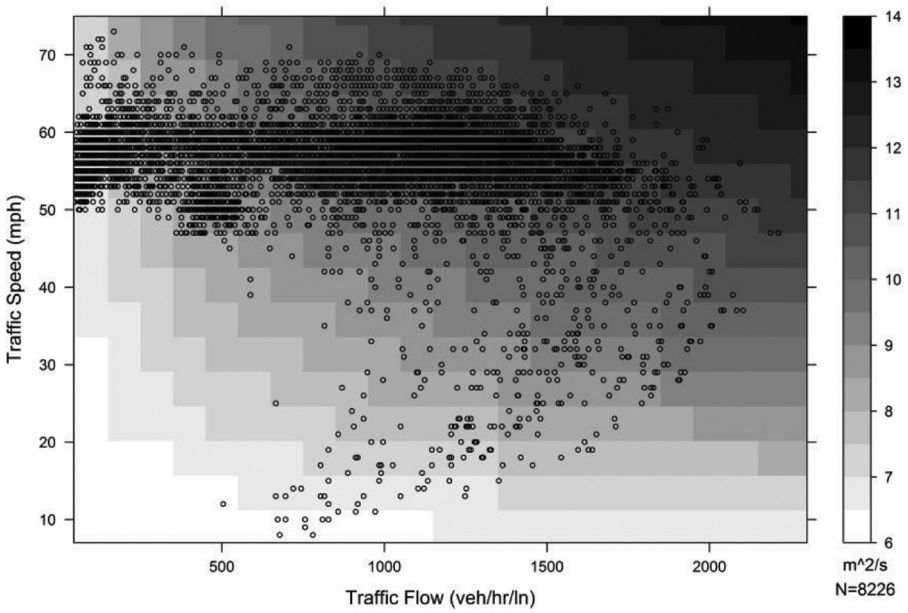

Fig. 4. Modeled roadway dispersion as shading on the traffic state (speed vs. flow) plane with illustrative traffic data; dispersion is lowest in heavy congestion.

traffic with moderate to high speeds (other things being equal). In heavy congestion with lower speeds, dispersion d_j is lower and emissions rates e_j are higher, but these exposure-increasing effects are mitigated by lower traffic flows q_j. The partially offsetting effects of these model variables (q_j, d_j, and e_j) in changing traffic conditions help explain why exposure intensity plays a weaker role than exposure duration in determining total inhalation during congestion (Section 3.2).

Linear regression shows that d_j increases $0.00086\,m^2/s$ with each veh/hr of q_j, $0.055\,m^2/s$ with each mph of v_j, and $1.52\,m^2/s$ with each m/s of wind speed u by method (1)—all significant at $p < 0.01$, $R^2 = 0.46$. Using the method (2) estimates, d_j increases $0.00079\,m^2/s$ with each veh/hr of q_j and $0.071\,m^2/s$ with each mph of v_j—also significant at $p < 0.01$, $R^2 = 0.94$. The correlations in Table 5 show that estimates of dispersion d_j are more closely linearly related to traffic flow q_j than traffic speed v_j. Although q_j explains more of the variance in d_j than v_j for both methods of estimating d_j, u is the dominant factor for method (1) estimates of d_j.

Besides traffic variables, other influences on estimates of d_j include the fraction of HD vehicles and the number of lanes. Using base conditions of a three-lane road with 55 mph traffic at 1,000 veh/hr/ln and the same fixed wind of method (2), d_j increases 11% if the percentage of HD vehicles on the road is increased from 8.7% to 15% HD, and d_j decreases 6% if the fraction of HD vehicles is decreased to 5% HD. Increasing the number of lanes from three to four increases d_j by 12%, and decreasing the number of lanes from three to two decreases d_j by 13%. A rotation of wind angle from 135° to 90° with respect to the roadway increases d_j by 23%. In comparison, an increase in traffic flow from 1,000 to 1,500 veh/hr/ln increases d_j by 9%. While traffic conditions do impact dispersion estimates, other factors (especially wind) could be more influential. The sensitivity of d_j to these factors reveals other potential offsetting effects for dispersion, where more HD vehicles or more lanes of roadway (with a commensurate increase in vehicle volume) would increase both total emissions ($e_j \cdot q_j$) and dispersion (d_j).

3.4. *Vehicle Penetration*

As stated in Section 2.5, it is possible that vehicle penetration of pollutants increases with vehicle speed, though data are insufficient to implement in this model. As an exploration of the potential effects of increasing p_j with v_j, consider a linear model where p_j increases from 0.54 at 20 mph to 0.64 at 70 mph (extracted from Xu and Zhu (2009) for 50 nm particulate matter with the vehicle's fan and recirculation off). For the simulated trips in this paper the result is a mean p_j of 0.607. The estimated p_j by this approach are negatively correlated with segment exposure intensity, with a correlation coefficient between p_j and i_j^t of −0.15 for CO and −0.28 for NO_x using the method (1) estimates. Using method (2), the correlation coefficients between p_j and i_j^t are −0.62 and −0.58 for CO and NO_x, respectively.

Because of the negative correlation, varying p_j would lower exposure intensity more for the higher-exposure motorists. Thus, varying p_j introduces another offsetting effect of traffic that dampens the increase of exposure intensity in congestion, similar to lower q_j in congestion as discussed in Section 3.3. For this reason, assuming constant p_j is conservative with respect to the finding that exposure duration is the primary effect of traffic on exposure. Further still, the amount of error associated with a constant p_j is small: there is a correlation coefficient of 0.997 between trip inhalation estimates made with the varying p_j and with a fixed p_j at the mean value of 0.607. A steeper slope on the $p_j = f(v_j)$ line would lead to more error from using a constant

p_j, but would also further offset increased exposure intensity in congestion. Simply lowering p_j in a way that is not a function of the traffic speed (for example from 1.0 to 0.6) will scale the estimated inhalation but not affect the main findings of this study. In other words, a uniform reduction in penetration can reduce total exposure, but the comparative impacts of congestion on exposure intensity and duration would be unchanged.

4. Discussion

The modeling approach of this study allows isolation of traffic effects on exposure, which can be masked by the dominating influence of varying wind and background concentration conditions. But as a modeling study it necessarily employs simplifying assumptions and parameter estimates. This research uses a deterministic model and general results are based on expected values. However, to analyze the impact of parameter variability, additional research is necessary to formulate and analyze this problem as a stochastic model. As illustrated in Section 3.2, including the exogenous influences of background concentrations and wind reduces the statistical strength of the relationships between traffic conditions and exposure. The modeled congestion impacts can be altered when accounting for uncertainty by including other, unobserved exogenous influences that would further reduce the statistical relationships; if the variability introduced by exogenous stochastic processes were sufficiently large, it could render the traffic variables insignificant. This observation serves as (1) a caveat on the study results (the total effect of traffic congestion level may be insignificant, meaning that the relative importance of the intensity and duration effects of congestion may be irrelevant in some scenarios), (2) a motivation for the study design (showing the analytical benefit of isolating traffic variables), and (3) support for the finding that nontraffic factors (i.e., background concentrations and wind) are the dominant influences on total inhalation through changing exposure intensity.

Parameter uncertainty especially applies to the dispersion estimates, which make use of a statistical approximation of the vertical distribution of pollutant concentrations. Although the selected parameter values are considered reasonable for this study, large variability would exist regarding the parameters in a specific location, and some parameters (breathing rate and vehicle penetration, for example) would vary by motorist or vehicle. Despite the uncertainty of the estimates, the analysis in this paper is useful in elucidating trends and relationships among traffic-related variables that impact motorists' inhalation of on-road pollution.

Equation 3 is useful for assessing the effect of adjusting study parameters. For example, changing vehicle penetration p_j or breathing rate r in a way that is not a function of the traffic state (v_j or q_j) will simply scale the estimated exposure without changing the main findings of the study. Increasing the background concentrations b_j will lessen the influence of traffic conditions on total inhalation, but will not change the essence of the findings either. Decreasing b_j will have the opposite effect, amplifying the influence of traffic. Other parameters such as the assumed receptor height z will also have an effect on the estimated exposure, but as long as they do not correlate with the traffic variables q_j or v_j, the effect will be similar to that for the breathing rate r: changing estimated inhalation without materially changing the findings. The fraction of HD vehicles is a potentially important traffic-related parameter that would influence both emissions and dispersion estimates because of large differences between LD and HD vehicles (Table 1 and Bigazzi and Figliozzi [2013]). Further effects of varying HD vehicle presence are left as a topic for future study.

The use of a single dispersion parameter simplifies the discussion of traffic effects but might not be appropriate in traffic conditions where insufficient roadway mixing occurs. If a vehicle queue is sufficiently slow and atmospheric turbulence is low, individual vehicles' emissions plumes in the roadway might not be well mixed, leading to high spatial and temporal variability of on-road concentrations. Whether the average motorist's total exposure would be the same as in a well-mixed roadway air mass is not known, and would probably require development of new on-road dispersion models to answer. If cross-road advection does not dominate dispersion, horizontal vehicle-induced turbulence (not modeled here) could be a dominant factor in evolving roadway concentrations. A further complication would exist if turbulent kinetic energy vehicle wakes are not independent, in which case extremely detailed trajectory data for each vehicle would be required to model the cumulative vehicle-induced roadway turbulence (assuming the plume-interaction relationships are known). These questions require further investigation of on-road dispersion processes to assess.

This paper is unique in isolating and assessing the mechanics of how short-term traffic states are expected to impact motorists' trip exposure, including vehicle-induced dispersion. The finding that traffic effects on exposure intensity can be obscured by exogenous factors agrees with empirical research by Fruin et al. (2008), who found measured in-vehicle concentrations of several pollutants to be poorly correlated with traffic speed and volume. They hypothesize that a likely reason is "offsetting effects" of vehicle density and dispersion, which is supported by the present study. Some studies have found significant correlations between measured in-vehicle pollution concentrations and an aggregate measure of vehicle traffic (Kaur, Nieuwenhuijsen, and Colvile 2007; Koushki, Al-Dhowalia, and Niaizi 1992; Zagury, Moullec, and Momas 2000), but the traffic measure is usually long-term vehicle counts (one hour or more), and so fundamentally different from the short-term traffic states analyzed here.

Finally, the trip exposure results in this paper are presented with respect to varying departure times, not the number of motorists. For a population perspective, the trip exposures would need to be weighted by travel volumes throughout the day. A broader perspective of the role of traffic congestion in overall daily exposure would also need to consider alternative exposure environments, congestion

effects on travel decisions such as mode choice and land use patterns, and travel delay effects on daily time allocation.

5. Conclusions

The modeling results in this paper show that trip-total inhalation of traffic-related CO and NO_x pollution is expected to increase for motorists in traffic congestion. Considering only traffic effects, model results show that exposure duration (i.e., motorist delay) is the primary influence of traffic congestion level on mass inhalation over a freeway trip. Exposure intensity also increases in congestion, but is less correlated with traffic conditions than exposure duration. Considering nontraffic factors, varying wind and background concentrations are the dominant influences on total inhalation through changing exposure intensity, and are sufficient to obscure the effects of traffic on exposure intensity. Uncertainty in the modeling means that factors other than congestion level could be even more important for trip-total exposure. The variability introduced by stochastic processes could be sufficiently large to make the expected differences between the exposure duration and exposure intensity effects of congestion insignificant. Additional research is needed to explore this point with a stochastic model.

Variability in exposure intensity with changing traffic conditions is mitigated by offsetting impacts among traffic flow, emissions rates, and pollutant dispersion. Exposure intensity increases with traffic flow and decreases with higher traffic speed, although traffic flow has a stronger relationship with exposure intensity than traffic speed does. Heavy congestion with low average speeds has lower-than-maximal vehicle flows. This combination leads to long exposure duration, high emissions rates, and low pollutant dispersion—but not maximal total emissions. The distribution of exposure duration along a corridor also changes in congestion, intensifying the importance of exposure "hot spots" at traffic bottlenecks. Although vehicle penetration is not varied in this model, the expected impact on the findings is small, because varying vehicle penetration with speed would offset increased roadway concentrations in congestion.

Assessing the effects of traffic management on motorists' exposure requires consideration of both intensity and duration impacts. The findings in this paper suggest that *traffic-based* exposure mitigation should focus on reducing travel times through reduced vehicle flows (demand-side congestion mitigation) rather than through increased vehicle throughput capacity (supply-side congestion mitigation). Decreasing travel time by increasing vehicle throughput can have the detrimental effect of increasing total emissions. Further, congestion mitigation that only increases travel speeds without reducing vehicle volumes will not substantially reduce exposure for anyone outside of the congested traffic stream.

Exposure intensity can also be reduced by other strategies not considered in this analysis because of the paper's focus on traffic congestion characteristics (Section 2.7). Improvements in engines and fuels can reduce emissions intensity per vehicle-mile of travel and improvements in vehicle design can reduce penetration and improve removal of pollutants in the cabin, both of which will decrease exposure intensity for motorists. These effects, if independent of congestion level, will simply scale down traffic impacts without changing the findings of the paper. The main exception would be if the impacts of traffic characteristics were muted to the point of insignificance (making any intensity/duration effect difference irrelevant). If a change in vehicle technology made a parameter more or less sensitive to congestion, then the effects of congestion on exposure intensity and duration could be affected as well (similar to Section 3.4). One example would be an advanced vehicle fleet with less emissions rate sensitivity to stop-and-go traffic because of hybrid engine technology with regenerative braking. Such a change would likely *increase* the relative importance of exposure duration by reducing the emissions rate (and thus exposure intensity) effects of changing congestion levels.

Comparing estimated on-road exposure to background concentrations, corridor management can be an important part of traveler exposure mitigation for a reactive pollutant such as NO_x, which is almost five times higher than background levels in this study. Estimated on-road exposure is 41% higher than background levels for CO. But individual trip CO exposures range up to 36 times higher than background levels, illustrating the importance of location-targeted traveler exposure mitigation.

Motorist delay is less deleterious when spent on low-flow segments than on high-flow segments, so a travel time shift to lower-flow facilities could reduce motorist pollution inhalation, even with the same travel time. Distributing vehicle traffic over lower-volume streets could lead to less pollution inhalation for motorists than concentrating travelers on high-volume facilities such as freeways, but it will affect pollution exposure for nonmotorists and nontravelers as well, which must also be considered. On an individual scale, motorists can greatly reduce their own exposure during travel by adjusting their departure time to less congested periods, or by improving their vehicle cabin protection (reducing penetration of pollutants).

Acknowledgments

The authors would like to thank for their support of this project: the Oregon Transportation Research and Education Consortium (OTREC), the U.S. Department of Transportation (through the Eisenhower Graduate Fellowship program), and the U.S. National Science Foundation (through the Graduate Research Fellowship Program, Grant No. DGE-1057604). Additionally, thanks are given to the anonymous reviewers who provided valuable feedback for improvement of this paper.

References

Baumer D, Vogel B, Fiedler F. 2005. A new parameterisation of motorway-induced turbulence and its application in a numerical model. Atmospheric Environment 39(31):5750–5759.

Benson P. 1992. A review of the development and application of the CALINE 3 and 4 models. Atmospheric environment. Part B, Urban atmosphere 26(3):379–390.

Bigazzi AY, Figliozzi MA. 2012. Impacts of freeway traffic conditions on in-vehicle exposure to ultrafine particulate matter. Atmospheric Environment 60:495–503.

Bigazzi AY, Figliozzi MA. 2013. The role of heavy-duty freight vehicles in reducing emissions on congested freeways with elastic travel demand functions. Transportation Research Record: Journal of the Transportation Research Board 2340:84–94.

Bigazzi AY, Siri H, Bertini R. 2010. Effects of temporal data aggregation on performance measures and other intelligent transportation systems applications. Transportation Research Record: Journal of the Transportation Research Board 2160:96–106.

Clifford MJ, Clarke R, Riffat SB. 1997. Local aspects of vehicular pollution. Atmospheric Environment 31(2):271–276.

de Nazelle A, Rodríguez DA, Crawford-Brown D. 2009. The built environment and health: Impacts of pedestrian-friendly designs on air pollution exposure. Science of the Total Environment 407(8): 2525–2535.

Eskridge RE, Rao ST. 1986. Turbulent diffusion behind vehicles: Experimentally determined turbulence mixing parameters. Atmospheric Environment (1967) 20(5): 851–860.

Fruin SA, Westerdahl D, Sax T, Sioutas C, Fine PM. 2008. Measurements and predictors of on-road ultrafine particle concentrations and associated pollutants in Los Angeles. Atmospheric Environment 42(2):207–219.

George LA, Parra J, Sitbon P. 2005. Horizons—Portland Area Real-Time and Archived Air Quality and Meteorological Data. Portland, OR: Center for Environmental Atmospheric Research (CEAR), Portland State University.

Gordon M, Staebler RM, Liggio J, Li S-M, Wentzell J, Lu G, Lee P, Brook JR. 2012. Measured and modeled variation in pollutant concentration near roadways. Atmospheric Environment 57: 138–145.

Gulliver J, Briggs DJ. 2005. Time-space modeling of journey-time exposure to traffic-related air pollution using GIS. Environmental Research 97(1):10–25.

Han X, Naeher LP. 2006. A review of traffic-related air pollution exposure assessment studies in the developing world. Environment International 32(1):106–120.

HEI Panel on the Health Effects of Traffic-Related Air Pollution. 2010. Traffic-Related Air Pollution: A Critical Review of the Literature on Emissions, Exposure, and Health Effects (Special Report 17). Boston, MA: Health Effects Institute.

Kalthoff N, Bäumer D, Corsmeier U, Kohler M, Vogel B. 2005. Vehicle-induced turbulence near a motorway. Atmospheric Environment 39(31):5737–5749.

Kanda I, Uehara K, Yamao Y, Yoshikawa Y, Morikawa T. 2006. A wind-tunnel study on exhaust-gas dispersion from road vehicles—Part II: Effect of vehicle queues. Journal of Wind Engineering and Industrial Aerodynamics 94(9):659–673.

Kastner-Klein P, Berkowicz R, Plate EJ. 2000. Modelling of vehicle-induced turbulence in air pollution studies for streets. International Journal of Environment and Pollution 14(1):496–507.

Kaur S, Nieuwenhuijsen MJ, Colvile RN. 2007. Fine particulate matter and carbon monoxide exposure concentrations in urban street transport microenvironments. Atmospheric Environment 41(23): 4781–4810.

Kim B, Wayson R, Fleming G. 2006. Development of Traffic Air Quality Simulation Model. Transportation Research Record: Journal of the Transportation Research Board 1987:73–81.

Kono H, Ito S. 1990. A micro-scale dispersion model for motor vehicle exhaust gas in urban areas—OMG volume-source model. Atmospheric Environment. Part B. Urban Atmosphere 24(2):243–251.

Koushki PA, Al-Dhowalia KH, Niaizi SA. 1992. Vehicle occupant exposure to carbon monoxide. Journal of the Air & Waste Management Association 42(12):1603–1608.

May A. 1989. Traffic Flow Fundamentals. Upper Saddle River, NJ: Prentice Hall.

McNabola A, Broderick BM, Gill LW. 2008. Relative exposure to fine particulate matter and VOCs between transport microenvironments in Dublin: Personal exposure and uptake. Atmospheric Environment 42(26):6496–6512.

McNabola A, Broderick BM, Gill LW. 2009. The impacts of inter-vehicle spacing on in-vehicle air pollution concentrations in idling urban traffic conditions. Transportation Research Part D: Transport and Environment 14(8):567–575.

O'Donoghue RT, Gill LW, McKevitt RJ, Broderick B. 2007. Exposure to hydrocarbon concentrations while commuting or exercising in Dublin. Environment International 33(1):1–8.

Oregon Department of Transportation, 2010. Traffic volumes and vehicle classification. http://highway.odot.state.or.us/cf/highwayreports/traffic_parms.cfm (accessed 3 November 2010).

Pasquill F. 1983. Atmospheric Diffusion: The Dispersion of Windborne Material from Industrial and Other Sources. 3rd ed. UK: Ellis Horwood.

Rao KS. 2002. ROADWAY-2: A model for pollutant dispersion near highways. Water, Air, & Soil Pollution: Focus 2(5):261–277.

Rao KS. Gunter RL, White JR, Hosker RP. 2002. Turbulence and dispersion modeling near highways. Atmospheric Environment 36(27):4337–4346.

U.S. EPA, 2009. Motor Vehicle Emission Simulator (MOVES) 2010 User's Guide (No. EPA-420-B-09–041). Washington, DC: U.S. Environmental Protection Agency.

Wang JS, Chan TL, Cheung CS, Leung CW, Hung WT. 2006. Three-dimensional pollutant concentration dispersion of a vehicular exhaust plume in the real atmosphere. Atmospheric Environment 40(3):484–497.

Wang Z, Liu C. 2005. An empirical evaluation of the loop detector method for travel time delay estimation. Journal of Intelligent Transportation Systems 9(4):161–174.

Wijnen JH, Verhoeff AP, Jans HW, Bruggen M. 1995. The exposure of cyclists, car drivers and pedestrians to traffic-related air pollutants. International archives of occupational and environmental health 67(3):187–193.

Xu B, Zhu Y. 2009. Quantitative analysis of the parameters affecting in-cabin to on-roadway (I/O) ultrafine particle concentration ratios. Aerosol Science and Technology 43(5):400–410.

Zagury E, Moullec YL, Momas I. 2000. Exposure of Paris taxi drivers to automobile air pollutants within their vehicles. Occupational and Environmental Medicine 57(6):406–410.

Zhu Y, Eiguren-Fernandez A, Hinds WC, Miguel AH. 2007. In-cabin commuter exposure to ultrafine particles on Los Angeles freeways. Environmental Science & Technology 41(7):2138–2145.

Appendix

Notation

Symbol	Variable	Unit
b_j	Background concentration during travel on road segment j	g/m^3
c_j	Total exposure concentration on road segment j	g/m^3
ϵ_z	Total turbulent kinetic energy contributing to vertical dispersion	m^2/s^2
ϵ_z^{veh}	Vehicle-induced turbulent kinetic energy contributing to vertical dispersion	m^2/s^2
ϵ_z^{atm}	Atmospheric turbulent kinetic energy contributing to vertical dispersion	m^2/s^2
e_j	Pollution emissions rate for vehicles on road segment j	g/veh-mi
d_j	Dispersion parameter on road segment j	m^2/sec
f_λ	Fraction of vehicle flow of class λ	—
λ	Vehicle class designator	—
$\hat{\lambda}$	Set of characteristics for vehicles of class λ {height, width, length, drag coefficient}	{m, m, m, —}
Λ	Set of vehicle classes {light-duty, heavy-duty}	—
h	Emissions line-source height	m
H	Composite vehicle height	m
I	Total mass inhalation over all road segments	g
i_j^t	Temporal inhalation rate on road segment j	g/hr
$\overline{i^t}$	Average temporal inhalation rate over all road segments	g/hr
i_j^s	Spatial inhalation rate on road segment j	g/mi
l_j	Length of road segment j	mi
N	Number of lanes	—
p_j	Vehicle penetration on road segment j	—
q_j	Traffic flow on road segment j	veh/hr
r	Breathing rate	m^3/hr
σ_z	Statistical approximation of the plume height	m
s_j	Travel speed on road segment j	mi/hr
θ_j	Wind angle with respect to the roadway on road segment j	degrees
τ	Residence time of traffic-emitted pollutants in the roadway	s
s_j	Travel speed	mi/hr
t_j	Travel time on road segment j	hr
T	Total travel time over all road segments	hr
u	Wind speed	m/s
v_j	Traffic speed on road segment j	mi/hr
$w'^2_{xy,\lambda}$	Vertical TKE at location (x,y) due to the wake of a vehicle of class λ	m^2/s^2
w'^2_λ	Total vertical TKE on the roadway due to the wake of a vehicle of class λ	m^2/s^2
W	Width of a single lane	m
x	Distance from the vehicle centroid perpendicular to the direction of travel	m
y	Distance behind the vehicle centroid parallel to the direction of travel	m
z	Receptor height	m